A Comparative Assessment of Multi-criteria Decision Analysis for Flood Susceptibility Modeling

Ehsan Shahiri Tabarestani
Iran University of Science and Technology
Hossein Afzalimehr (hafzali@iust.ac.ir)
Iran University of Science and Technology

Research Article

Keywords: Flood susceptibility map, GIS, MABAC method, Multi-criteria decision-making analysis, ROC

Posted Date: March 22nd, 2021

DOI: https://doi.org/10.21203/rs.3.rs-202961/v1

A comparative assessment of multi-criteria decision analysis for flood susceptibility modeling

Ehsan Shahiri Tabarestani, Hossein Afzalimehr *

Ph.D. student, Department of Civil Engineering, Iran University of Science and Technology, Tehran, Iran, ehsan_shahiri@yahoo.com

*Professor, Department of Civil Engineering, Iran University of Science and Technology, Tehran, Iran, hafzali@iust.ac.ir

Abstract

Floods are one of the most damaging natural disasters throughout the world. The purpose of this study is to develop a reliable model for identification of flood susceptible areas. Three Multi-criteria decision-making techniques, namely Analytical Hierarchy Process (AHP), Technique for Order of Preference by Similarity to Ideal Solution (TOPSIS), and Attributive Border Approximation Area Comparison (MABAC) methods combined with weight of evidence (WOE) were used in Mazandaran Province, Iran. MABAC method is applied to determine the flood susceptibility in this study, for the first time. At first, 160 flood locations were identified in the study area, of which 112 (70%) locations were selected randomly for modeling, and the remaining 48 (30%) locations were used for validation. Using Geographic Information System (GIS) with eight conditioning factors including rainfall, distance from rivers, slope, soil, geology, elevation, drainage density, and land use, the flood susceptibility maps were prepared. The results showed that the area under receiver operating characteristic curve (AUROC) for the test data of AHP-WOE, TOPSIS-WOE-AHP, and MABAC-WOE-AHP methods were 75.3%, 91.6%, and 86.1%, respectively, which indicate the reasonable accuracy of models. High accuracy of the proposed new model (MABAC) clarifies its applicability for preventive measures.

Keywords: Flood susceptibility map; GIS; MABAC method; Multi-criteria decision-making analysis; ROC

1. Introduction

Among various natural disasters, floods are one of the most devastating cases, causing many damages and human losses in the world (Youssef et al. 2011). One of the preventive measures for flood hazards is preparing flood susceptibility mapping (Dang et al. 2011; Bubeck et al. 2012). By matching flood susceptibility maps with land use maps, it is possible to identify endangered areas, including cities, villages, bridges, factories, etc., to take the necessary measures to protect them.

GIS and remote sensing (RS) techniques provide an application in the natural disaster risks analysis (Haq et al. 2012; Jaafari et al. 2014). Therefore, these techniques have been proposed to evaluate flood hazard zoning in many studies (Dewan et al. 2007; Pradhan et al. 2011; Kazakis et al. 2015).

Some of the most common approaches for flood susceptibility modeling are artificial neural networks (Park et al. 2013; Radmehr and Araghinejad 2014), decision trees (Yeon et al. 2010; Khosravi et al 2018), fuzzy logic (Bui et al. 2012; Ramazi and Amini 2014), frequency ratio (Lee et al. 2012; Rahmati et al. 2015), weights of evidence (Tehrany et al. 2015; Khosravi et al 2016), analytical hierarchy process (Meyer et al. 2009; Zou et al. 2013), and logistic regression (Pradhan et al. 2008; Choi et al. 2012).

Multi-criteria decision analysis (MCDA) has been identified as an essential tool for analyzing complicated decision problems, that include incomparable data or criteria (Hwang & Yoon 1987; Malczewski 2006). AHP (Saaty 1977) is a popular method of multi-criteria decision-making (Pourghasemi et al. 2012), based on experts' knowledge in assigning weights. The efficiency of MCDA and GIS was assessed by Fernandez and Lutz (2010) for mapping the flood-susceptible areas in Tucuman Province, Argentina. They showed that the AHP method in GIS environment is a powerful technique to generate disaster hazard maps with a reasonable accuracy. Zou et al. (2013) recognized AHP technique as an understandable, convenient and cost-effective method for flood hazard evaluation. Subramanian and Ramanathan (2012) indicated that the AHP technique is suitable for regional researches. Other techniques in the field of MCDA for evaluating natural disaster risks are Technique for Order of Preference by Similarity to Ideal Solution (TOPSIS) and Multi-Attributive Border Approximation Area Comparison (MABAC). TOPSIS has been increasingly applied in flood hazard assessment because of its ability to deal with multiple attributes (Brito and Evers 2016). Mojtahedi and Oo (2016) developed the combination of a resampling bootstrap technique and TOPSIS to determine the flood hazard of Australia's states. Zhu et al. (2018)

used a TOPSIS-based approach for reservoir flood control operation. In another study, Luu et al. 2019 applied the new multiple linear regression-TOPSIS for Vietnam's flood risk assessment. The fuzzy-TOPSIS method has been used for flood risk evaluation in several researches (Jung et al. 2011; Lee et al. 2014). On the other hand, MABAC is one of the newest multi-criteria decision analysis methods, which developed at the Belgrade defense university research center (Pamucar and Cirovic 2015). A few studies were carried out in different fields using MABAC method (Gigovic et al. 2016; Liang et al. 2019). This method has not been used for flood hazard assessment, yet and it is new in flood susceptibility modeling.

The Mazandaran Province in Iran is always exposed to severe flood hazards, due to climatic and geographical conditions and extensive rainfall. The conversion of forest and agricultural lands into residential areas and increasing urbanization lead to an imbalance in the hydrological processes (Khosravi et al. 2016; Sadeghi-pouya et al. 2017).

While, all papers highlighted that each model has its limitation and there was no universal guideline to choose the best model in a region, combining several models may result in higher accuracy (Shafapour Tehrany et al. 2017; Hong et al. 2018; Costache, 2019; Rahman et al. 2019). MABAC method has not been applied for flood susceptibility assessment in the previous studies, yet, which means that this methodology lacks literature. Therefore, the purpose of present study is to evaluate the flood susceptibility through a novel hybrid model which was generated by the combination of MABAC, WOE, and AHP. As this method is a novel technique in flood assessment, this gap in this study was filled by determine the predictive power and comparing it to other hybrid methods (TOPSIS-WOE-AHP and AHP-WOE). The main reason for using these methods is to develop a high-performance model for estimating the flood potential in Mazandaran Province. For this purpose, the ROC Curve was used to validate and determine the accuracy of each model. Modeling and data processing were done in ARC-GIS 10.5 environment.

2. Study area

This study is located in the Mazandaran Province, with an area of approximately 23833 km^2 that occupied about 1.46% of Iran. The study area lies between the latitude of $35^\circ 46'$ to $36^\circ 58'$ N, and the longitudes of $50^\circ 21'$ to $54^\circ 8'$ E. The area's minimum elevation is -40 m, and the maximum is 5595 m above sea level. The average annual rainfall is about 520 mm and the rainiest months are March and April. Mazandaran province includes a series of

rivers that originate from the northern heights of Alborz Mountain and flow into the Caspian Sea. Most of the current rivers are permanent.

Land use patterns include rangeland (mostly in the height of more than 2000 m above sea), forests, garden lands, bare lands, and residential areas.

3. Methodology

3.1. Flood inventory map

The future flood event in a region can be predicted by analyzing the records of its occurrence (Manandhar 2010). A flood inventory map is the crucial factor in studying the relationship between flood events and different effective factors. In this research, a flood inventory map based on flood occurrence between 2012 and 2017 was prepared using Iranian Water Resources Department documentary sources and field surveys for Mazandaran Province. Flood locations were divided randomly into two datasets of training (almost 70%) and predicting (nearly 30%) data (Ohlmacher & Davis 2003; Pradhan 2010; Pourtaghi & Pourghasemi 2014; Khosravi et al. 2016). For this aim, 160 flood locations were identified in the study area, of which 112 (70%) locations were selected randomly for modeling, and the remaining 48 (30%) were used for validation. Map of Mazandaran Province, with flood locations is indicated in Fig. 1.

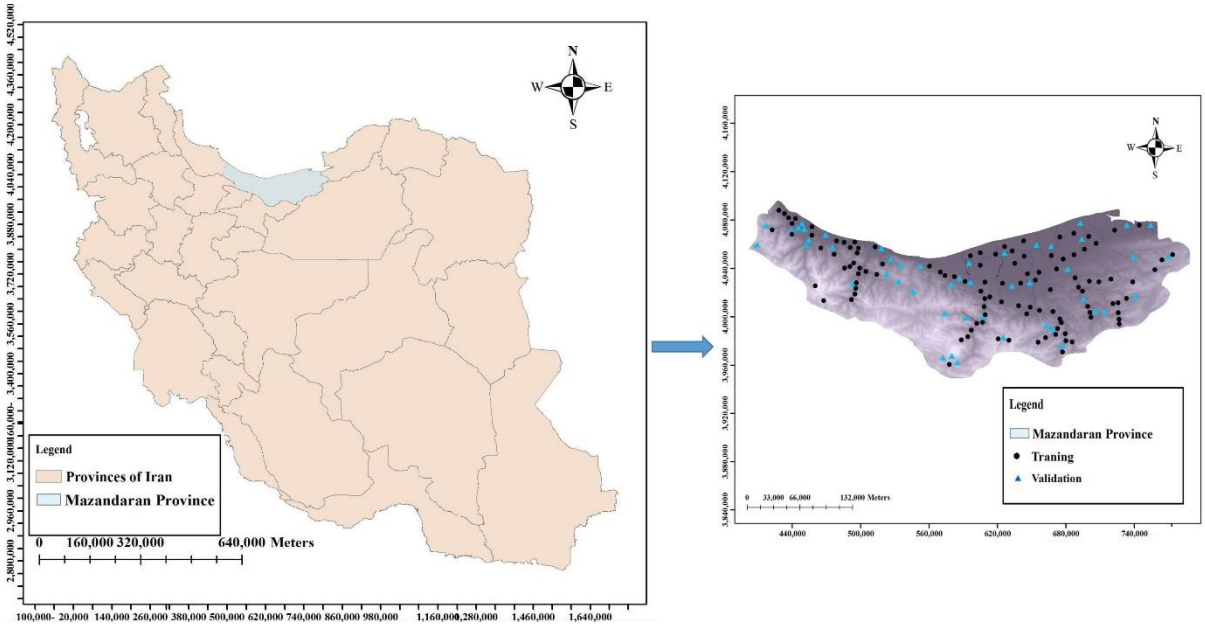

Fig. 1 Flood location map of Mazandaran Province, Iran

3.2. Flood conditioning factor

For preparing a flood susceptibility map, determining the flood conditioning factors is necessary (Kia et al. 2012). The flood conditioning factors were chosen by literature review, personal observation, experiences, and experts' knowledge (Kourgialas and Karatzas 2011; Ouma and Tateishi 2014; Suthirat et al. 2020; Ogato et al. 2020). Accordingly, rainfall, distance from streams, slope, soil, geology, elevation, drainage density, and land use were considered as important flood hazard factors in the Mazandaran Province. All the mentioned factors were converted to a raster grid with 30×30m grid-cells for application models.

Among these factors, the rainfall factor is the leading cause of flood in an area. For this factor, rainfall data for ten years (2008–2018) was collected at 15 stations. For interpolation of rainfall, different methods like ordinary kriging, simple kriging, spline, and Inverse Distance Weighted (IDW) with power of 1 to 5 were used. According to the Table 1, the lowest root mean square error (RMSE) and mean absolute error (MAE) were obtained for IDW method. Therefore, the map of rainfall has been produced by IDW with the power of 2 in ArcGIS software (Jahangir et al. 2019; Ogato 2020). Then to create a continuous raster rainfall data, it was converted to raster layer. To produce a spatial map of rainfall intensity, Fournier's index had been used by meteorological information of 15 hydrometric stations of Mazandaran Province from 2008 to 2018 as shown in Eq.1 (Morgan 2005).

$$MFI = \sum_{i=1}^{i=12} \frac{p_i^2}{P} \quad (1)$$

MFI is the modified Fournier index, Pi is the average monthly rainfall, and P is the average annual rainfall. This index shows the sum of the average monthly rainfall intensity at a station (Kourgialas and Karatzas 2011; Hernando and Romano 2015). A raster spatial rainfall map is shown in Fig. 2-a.

Table 1 Selection of the best method for interpolation of rainfall data

Interpolation method	RMSE	MAE
Simple kriging	137.6	113.4
Ordinary kriging	141.3	127.1
Spline	140.8	120.6
IDW: 1	138.1	122.3

IDW: 2	127.2	102.4
IDW: 3	140.2	115.5
IDW: 4	147.5	135.3
IDW: 5	159.1	124.1

Streams to pass the rainwater are vital factors that identify their density and distance from structures effective in predicting and reducing flood damage. Due to most villages in the study watershed in the river area, the amount of financial and human losses during floods reaches its maximum. The distance map in the ArcGIS environment was prepared using Euclidean Distant function from Spatial Analyst tools (Fig 2-b).

The slope factor has a significant role in the passing and stillness of surface waters. This factor is inversely related to the flood phenomenon. In ArcGIS software, the slope raster map was prepared using the digital elevation model (DEM) and slope generation tools (Fig. 2-c).

Soil attributes such as permeability, thickness, and infiltration rate directly affect the rainfall-runoff process (Rimba et al. 2017). The flood hazard increases with decrease in soil infiltration capacity, which causes an increase in surface runoff. When water is supplied at a rate more than the soil's infiltration capacity, it moves as runoff on sloping land, and can cause to flooding. There are some types of soil in study area, namely Chromic Vertisols, Inceptisols, Coastal Sands, Salt Flats, Water Body, Alfisols, Mollisols were, Rock Outcrops/Entisols, and Rock Outcrops/Inceptisols (Fig. 2-d).

Geological formations have an essential role in conducting or absorbing surface water due to their permeability. geology layer was classified into five groups: areas with impermeable rock layers, areas with clay soils - basalt - granite, areas with fine sand - mixed soils, areas with conglomerate-travertine-coarse-grained texture, and areas with gypsum-lime structure (Fig. 2-e).

The land use factor indicates the type of land can be a factor in accelerating or decelerating flood intensity. Land use change is one of the significant contributor to flooding, as urban expansion increases, impervious cover increases and forest cover decreases contributing to increased run-off (Hall et al. 2013). The land-use classes of the area were classified into five groups: urban-coastal areas, herbaceous plants - groves, fruit trees - agricultural lands, forest lands - agriculture, and finally, dense forest - mountainous areas (Fig. 2-f).

The elevation controls the movement of the overflow direction. The elevation raster map was produced using the digital elevation model (DEM) and slope generation tools in ArcGIS environment (Fig. 2-g).

Drainage density is defined as the ratio of the length of drainage per area. Drainage density is an inverse function of infiltration. In other words, greater drainage density shows high runoff for area and less prone to flood occurrences. The drainage map is overlaid on the basin map to determine the total length of streams to the basin's total area. Line density module was used to compute drainage density of the basin using the Spatial Analyst extension in ArcGIS.

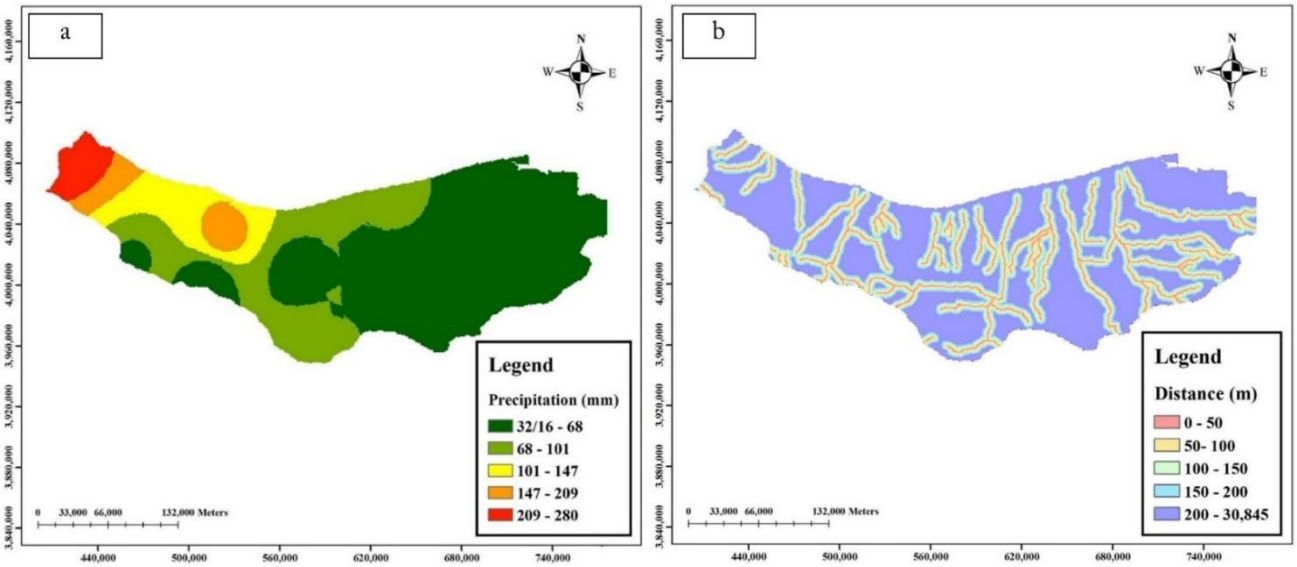

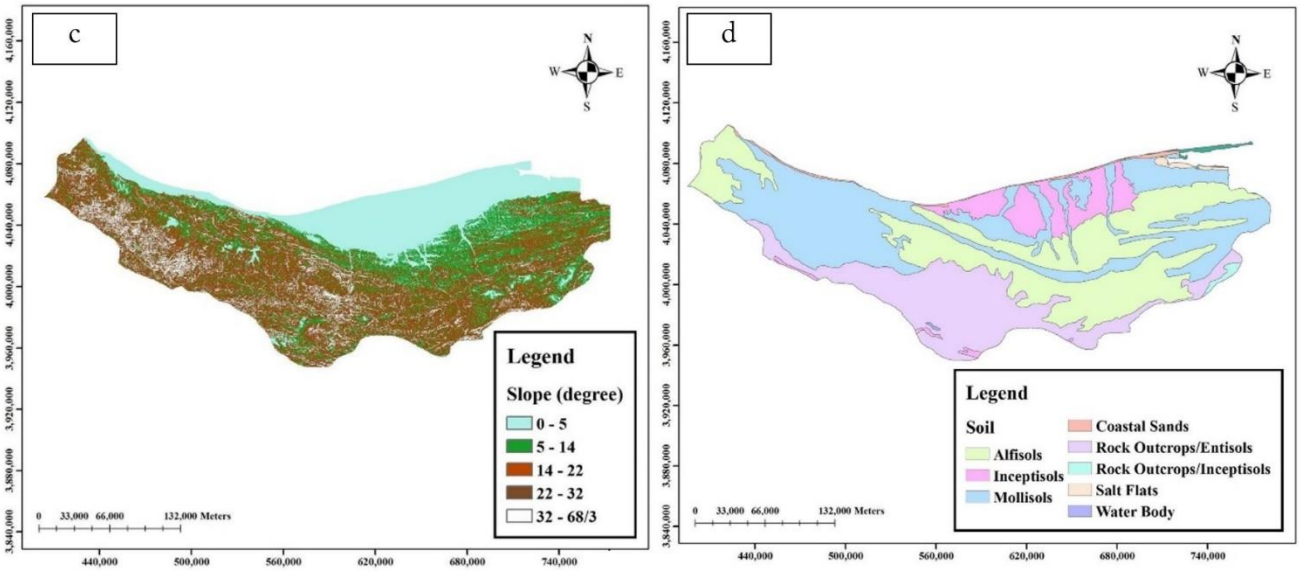
c
N
W
E
S
Legend
Slope (degree)
0 - 5
5 - 14
14 - 22
22 - 32
32 - 68/3
0 33,000 66,000 132,000 Meters
4,160,000
4,120,000
4,080,000
4,040,000
4,000,000
3,960,000
3,920,000
3,880,000
3,840,000
440,000
500,000
560,000
620,000
680,000
740,000
d
N
W
E
S
Legend
Soil
Alfisols
Inceptisols
Mollisols
Coastal Sands
Rock Outcrops/Entisols
Rock Outcrops/Inceptisols
Salt Flats
Water Body
0 33,000 66,000 132,000 Meters
4,160,000
4,120,000
4,080,000
4,040,000
4,000,000
3,960,000
3,920,000
3,880,000
3,840,000
440,000
500,000
560,000
620,000
680,000
740,000

147

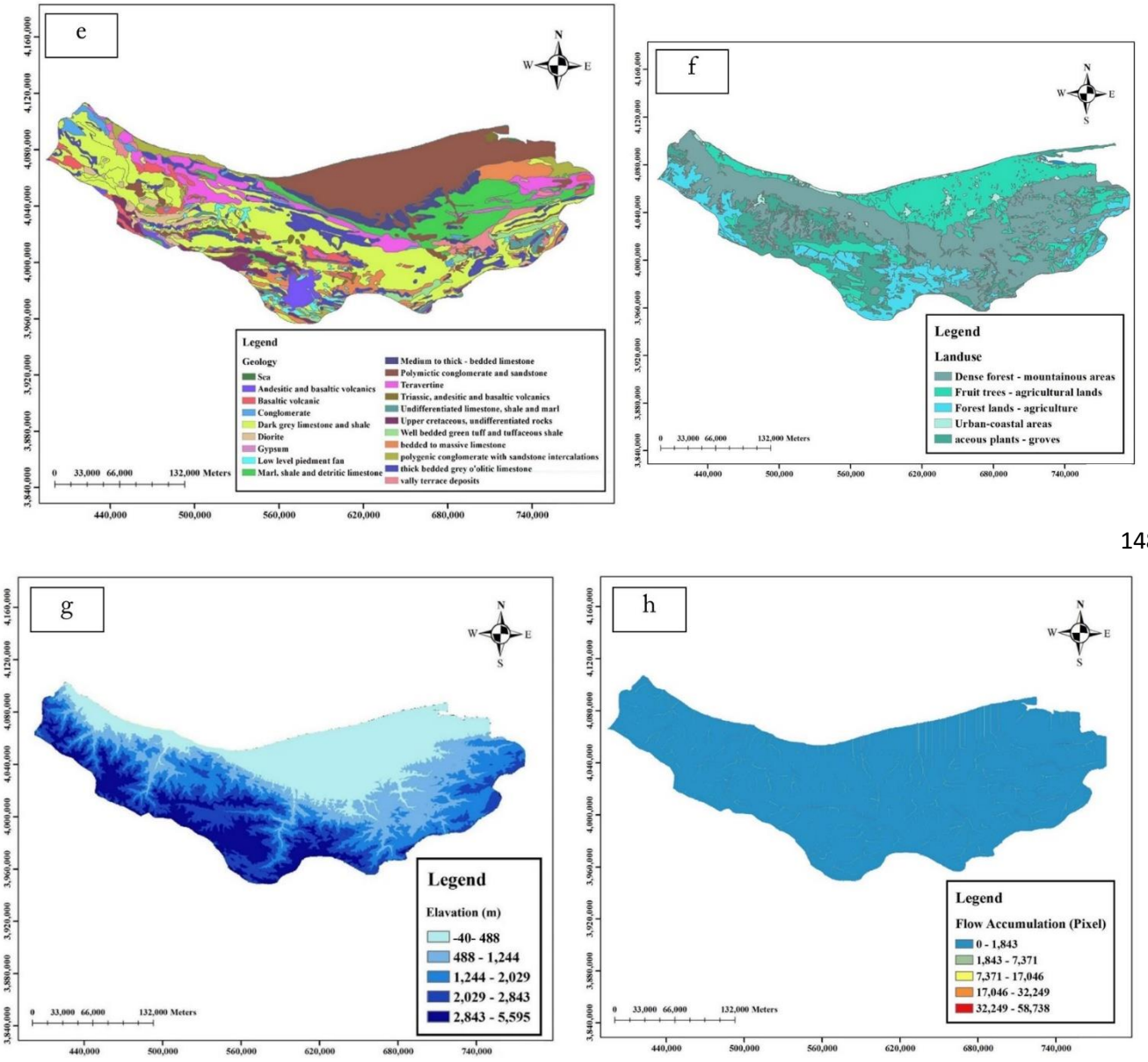

Fig. 2 Flood conditioning factors in the study area: (a) rainfall (b) distance from rivers (c) slope (d) soil type (e) geology (f) land use (g) elevation (h) flow accumulation

3.3 Flood susceptibility modeling

3.3.1 AHP model

Analytic hierarchy process established by Saaty (1977) is a technique for solving multiple criteria decision problems by setting their priorities. This method is implemented using the following steps:

At first, the pairwise comparison judgments were determined, using the nine-point scale (Saaty 1977). To make the matrix, each flood effective factor was rated in relation to the other factors, which were assigned values from 1/9 to 9 (Table 2). After that, all values from the pairwise comparison were normalized by dividing each entry in a column by adding all entries in that column to sum it to 1. Finally, to avoid any incidental judgment in the pairwise matrix, the consistency ratio (CR) was generated using the consistency index (CI) (Eq. 2, 3).

$$\mathrm{CI} = \frac{\lambda_{\max} - \mathrm{n}}{\mathrm{n} - 1} \quad (2)$$

Where $\lambda_{\max}$ is the largest eigenvalue of the pairwise comparison matrix and n is the number of factors.

$$\mathrm{CR} = \frac{\mathrm{CI}}{\mathrm{RI}} \quad (3)$$

where CI is the consistency index and RI is a random consistency index. The random consistency index of 1.45 is for the nine flood hazard factors (Saaty 1977). When the calculated CR was equal to (or less than) 10%, the estimated weighting coefficients were acceptable.

Table 2 Rating scale for the AHP pairwise comparison (Saaty 1977)

Description	Definition	Degree of importance
The two elements are equally important	Same importance	1
One element is relatively preferable to the other	Relative preference	3
One element is preferred over another	High preference	5
One element is much preferred over another	Too much preference	7
One element has a great advantage over the other.	Extremely high preference	9

3.3.2 WOE model

Weights of evidence method is based on log-linear Bayesian theory, which was first developed for mineral exploration in 1988 (Bonham-Carter et al. 1988). This bivariate statistical model can estimate the relationship between a flood occurrence and different conditioning factors by probability theory. It has been applied for

producing natural hazards susceptibility maps in several studies (Jaafari et al. 2014; Youssef et al. 2015; Khosravi et al. 2018). The model determines the weights of classes for each conditioning factor as follows (Bonhman-Carter et al. 1988):

$$W^+ = ln\frac{P(B|A)}{P(B|\bar{A})} \quad (4)$$

$$W^- = ln\frac{P(\bar{B}|A)}{P(\bar{B}|\bar{A})} \quad (5)$$

where P is probability, B is the presence, $\overline{B}$ is the absence of each effective factor. Also, A is the presence and $\overline{A}$ is the absence of flood, respectively (Xu et al. 2012). Weight contrast is the difference between W^+ and W^- .The magnitude of this contrast indicates the spatial correlation between the effective factors in the flood occurrence (Dahal et al. 2008). The value of C is positive and negative, for positive and negative relations respectively (Pourghasemi et al. 2013). Standard deviation for W is determined by Eq. 6:

$$S(C) = \sqrt{S^2W^+ + S^2W^-} \quad (6)$$

S^2W^+ and S^2W^- are the variance of positive and negative weights, respectively and calculated as follows:

$$S^2W^+ = \frac{1}{N(B \cap A)} + \frac{1}{B \cap \bar{A}} \quad (7)$$

$$S^2W^- = \frac{1}{N(\bar{B} \cap A)} + \frac{1}{\bar{B} \cap \bar{A}} \quad (8)$$

Where N denotes the number of unit cells. Finally the final weight (W_{final}) is expressed as follows:

$$W_{final} = C/S\,(C) \quad (9)$$

Where C is the contrast and S (C) is standard deviation.

3.3.3 MABAC model

MABAC model was first applied by Pamucar and Cirovic (2015) and developed at the Belgrade defense university research center for weight criteria and evaluation options. The casual relationship between the criteria is estimated using the modified fuzzy DEMATEL method. A DEMATEL method is a tool for visualizing the structure of complex casual relationships (Buyukozkan and Cifci 2011). Based on this method, criteria are divided into two categories of cause and effect. The extent of this effect is used to estimate the criteria' weight (Dalalah et al 2011). MABAC model consists of 6 important steps, as described below:

Step 1. Construction of the initial decision matrix (X)

In each problem, there are m alternatives and n criteria. Each of the options is displayed in the form of vectorization as $A_i = (x_{i1}.x_{i2}.x_{i3}.\ldots.x_{in})$ where x_{ij} specifies the status of the i option in the j criterion. Based on this, the initial decision matrix (X) is shown below.

$$X = \begin{bmatrix} x_{11} & x_{12} & x_{13} & \cdots & x_{1n} \\ x_{21} & x_{22} & x_{23} & \cdots & x_{2n} \\ \cdots & \cdots & \cdots & \cdots & \cdots \\ x_{m1} & x_{m2} & x_{m3} & \cdots & x_{mn} \end{bmatrix} \quad (10)$$

Step 2. Normalization of the initial decision matrix elements (N)

The decision matrix is normalized to neutralize the effect of the different scales of the criteria. Eq. 11 and 12 are used to normalize the positive and negative criteria, respectively.

$$n_{ij} = \frac{x_{ij} - x_i^-}{x_i^+ - x_i^-} \quad (11)$$

$$n_{ij} = \frac{x_{ij} - x_i^+}{x_i^- - x_i^+} \quad (12)$$

Where x_{ij}, x_i^+ and x_i^- are the elements of the initial decision matrix (X). x_i^+ and x_i^- are the maximum and minimum value of the observed criterion, respectively and defines as:

$$x_i^+ = \max(x_1.x_2.x_3 \ldots.x_m) \quad (13)$$

$$x_i^- = \min(x_1.x_2.x_3 \ldots.x_m) \quad (14)$$

Step 3. Calculation of a balanced normal decision matrix (V)

In this step, elements of balanced normal decision matrix are determined by Eq. 15.

$$v_{ij} = w_i \cdot (n_{ij} + 1) \quad (15)$$

Where v_{ij} are the elemnts of the balanced matrix (V), n_{ij} are the elements of the normalized matrix (N) and w_i is the weight coefficients of the criteria, which determined by AHP method in this study.

Step 4. Determination of the border approximation area matrix (G)

The border approximation area for each criterion is calculated by Eq. 16.

$$g_i = \left(\prod_{j=1}^{m} v_{ij} \right)^{\frac{1}{m}} \quad (16)$$

Where v_{ij} are the elements of the weighted matrix (V), and m is the total number of alternatives.

After determining the value of g_i for each criterion, a border approximation area matrix (G) is estimated according to Eq. 17.

$$G = [g_1 \ g_2 \ \ g_3 \dots g_n] \quad (17)$$

Where n is the total number of criteria according to selection of alternatives.

Step 5. estimation of the distance of the alternatives from the border approximation area (Q)

This distance is equal to the difference between the weighted matrix elements (V) and the value of the border approximation area matrix (G), as indicated in Eq. 18.

$$Q = V - G \quad (18)$$

After calculating the value of matrix Q, the belonging of each alternative can be specified.

The upper approximation area (G^+) is the region which consists of the ideal alternative (A^+), and the lower approximation area (G^-) is the region which consists of the anti-ideal alternative (A^-). The belonging of alternatives to the approximation area is determined based on Eq. 19.

$$A_i \in \begin{cases} G^+ & if \ \ q_{ij} > 0 \\ G & if \ \ q_{ij} = 0 \\ G^- & if \ \ q_{ij} < 0 \end{cases} \quad (19)$$

Based on MABAC method, in order to select the best alternative, it is essential for it to have as many criteria as possible belonging to the upper approximation area (G^+).

Step 6. Ranking the alternatives

In the final step of MABAC method, the value of criterion functions for each alternative is determined based on the sum of the distance of the alternatives from the border approximation area (q_i) as shown in equation 20.

$$S_i = \sum_{j=1}^{n} q_{ij} \qquad j = 1.2 \dots . n \ \ \ i = 1.2 \dots . m \quad (20)$$

Where n is the number of criteria, and m is the number of alternatives.

3.3.4 TOPSIS model

TOPSIS method was first proposed by Hwang and Yoon (1981). The basic principle is to calculate the distance between the evaluation object and the ideal solution and rank the evaluation object according to the distance

(Izadikhah et al. 2014). The ideal object was defined as the object closest to the positive ideal solution and also farthest from the negative ideal solution (Lin et al. 2008).

TOPSIS is a practical method that compares options according to the value of data in each weight of the criteria. The fuzzy TOPSIS method is more compatible than the non-fuzzy TOPSIS method due to fuzzy sets. The use of fuzzy function due to flexible composition and other integrated methods will lead to better results in flood zoning and provide results closer to reality. To determine a flood zoning map based on the AHP-TOPSIS method, the following steps are performed.

Step 1. Formation of initial decision matrix (X)

This matrix is the same as the initial decision matrix in the MABAC model.

Step 2. Normalization of the decision matrix (N)

To normalize the decision matrix, the division of each value by the root of the sum of squares of the values of the column element is used (Eq. 21).

$$r_{ij} = \frac{X_{ij}}{\sqrt{\sum_{i=1}^{m} X_{ij}^2}} \quad (21)$$

Where X_{ij} is the value of the decision matrix in column number i and row number j, and r_{ij} is the dimensionless value of this entry.

Step 3. Formation of a normal weighted matrix

In this step, the weight of the criteria obtained from the AHP method is multiplied by the normal matrix's values to obtain the weighted matrix.

Step 4. Finding the ideal and non-ideal solution

In this section, the criteria are divided into two groups of positive and negative. According to the study's purpose, the factors that increase the potential of flooding occurrence in the region are positive criteria including rainfall, drainage density, soil type, geology, and land use. In contrast, the factors that lead to a decrease in flood potential are negative criteria, including the distance from the streams, slope, and height.

Step 5. Calculation of the distance from the ideal and non-ideal solution

In this step, each pixel's distance from its positive and negative ideal is calculated (Eq. 22, 23).

$$d_i^+ = \sqrt{\sum_{j=1}^{n} \left(v_{ij} - v_j^+\right)^2} \quad (22)$$

$$d_i^- = \sqrt{\sum_{j=1}^{n} \left(v_{ij} - v_j^-\right)^2} \quad (23)$$

Where d_i^+ and d_i^- are distance from the ideal and non-ideal solution for pixel i, respectively, v_{ij}, is the value of pixel i corresponding to the criterion j, $v_j^+$and $v_j^-$are positive and negative ideal values of criterion j, respectively.

Step 6. Pixels ranking

The similarity index is determined using equation 16, and the score of each pixel is determined based on the AHP-TOPSIS method. The closer this index is to the number 1, Indicates higher pixel potential in terms of flood risk.

$$cl_i^* = \frac{d_i^-}{d_i^- + d_i^+} \quad (24)$$

3.4. Performance assessment

Validation of the prepared susceptibility maps is crucial in the identification and development flood-prone areas (Pourghasemi et al. 2014). In this study, the accuracy of the produced flood susceptibility maps by different models was verified using the Receiver Operating Characteristics (ROC). The ROC curve is a standard method to evaluate the result's accuracy and has been used by many researchers (Pradhan and Lee 2010a; Mohammady et al. 2012; Rahmati et al. 2014; Khosravi et al. 2018).

The ROC curve indicates the model's sensitivity to the percentage of pixels that were correctly predicted by the model versus the percentage of pixels predicted to total pixels. High sensitivity indicates many true predictions (true positives), while the high specificity shows a low number of false positives. In this curve, the false positive rate (1-specificity) is displayed on the X axis (Eq. 25) and the true positive rate (sensitivity) is displayed on the Y axis (Eq. 26) (Pourghasemi et al. 2014).

$$X = 1 - specifity = 1 - \left[\frac{TN}{TN + FP}\right] \quad (25)$$

$$Y = sensitivity = \left[\frac{TP}{TP + FN}\right] \quad (26)$$

The area under the curve (AUC) for testing data set describes how well the model predicts the flood occurrences (Pourtaghi and Pourghasemi 2014). The qualitative relationship between AUC and model's prediction accuracy can be classified into 5 classes as follows: 0.5–0.6 (poor); 0.6–0.7 (average); 0.7–0.8 (good); 0.8–0.9 (very good); and 0.9–1 (excellent) (Yesilnacar 2005).

4. Results

4.1. Flood susceptibility mapping

The results of prioritizing the effective factors in flooding using the AHP method and the relationship between flood occurrences and each class of effective factors using WOE model are presented in Table 3. As indicated, all of the quantitative and qualitative factors were classified into 5 classes based on natural breaks in the ArcGIS environment (Lin et al. 2020; Ogato et al. 2020). In the next columns, the number of flood pixels (training floods) and total pixels for each class were specified. Using WOE model, the final weight (Eq. 9) of each class was obtained. These weights imply the level of sensitivity of the classes to flooding.

According to the AHP analysis, among the eight effective factors in determining the flood potential, the rainfall, distance from rivers and slope with the weight of 0.349, 0.208, and 0.128 respectively, have the most impact on flood hazard (Fernandez and Lutz 2010; Youssef et al. 2011). On the other hand, geology, elevation, land use, flow accumulation and soil type factors ranked next. The calculated consistency ratio of pairwise comparison was 0.084 which was less than 0.1, so the estimated weighting coefficients were acceptable.

Floods occur mainly in rainy conditions. The results show that with increasing rainfall, the sensitivity of the floors to flooding increases. For rainfall factor, the last class including 209-280 mm had the highest C/Sc and the maximum impact on flooding, and the first 2 classes of rainfall, had negative impact on flood occurrences due to negative value. For the factor of distance from the rivers, the fourth and fifth classes with the lowest distance from rivers had the greatest influence on the occurrence of floods. After the distance of 100 m from the rivers, all classes had a negative impact on flooding. For the third effective factor or slope, the last (0-5) class had positive influence on the floods, however other classes had negative influences on flooding. It is clear that by increasing the slope, runoff flows rapidly and the probability of flooding decrease. The results of the soil parameter showed that the alficol soil group with a final weight of 0.425 had the highest value due to its hard and impermeable texture. In the

case of geology factor, the impermeable rock layers related to the Early Cretaceous period had the highest sensitivity to floods due to the low speed of water transfer to the groundwater with the highest score (4.511). Another important factor is elevation. the last two classes had the positive influence and the rest had the least influence on the occurrence of floods. It is indicated that with increasing the elevation, the sensitivity of the flooding decreases. The results of land use factor showed that the first two classes including dense forests, mountainous areas, forest and agricultural lands have negative impact on flooding and Herbaceous plants and groves have the highest weight (1.684). Although urban and rural areas have the highest level of flood risk, due to their great distance from the rivers, a small number of floods occurred in these areas. Therefore, the final weight indicates the low sensitivity of these areas on flooding occurrence. The results of drainage density parameter showed that areas with higher drainage density are more sensitive to the occurrence of flooding, so that the last class has the highest final weight (19.841).

After determining the weight of the effective factors in the occurrence of flood using AHP method and multiplying it by the weight of the mentioned factors, which was obtained using WOE method, according to Eq. 9, weight maps were collected and the final flood susceptibility map (FSM) of the study area was prepared in GIS environment. If the final weight of each factor class (last column of Table 3) is multiplied by the value of each pixel of MABAC and TOPSIS methods (Eq. 20, 24), the final flood susceptibility maps based on the MABAC-WOE-AHP and TOPSIS-WOE-AHP methods were prepared.

342

343

Table 3 relationship between flood conditioning factors and flooding locations 344

Factor	Class	No. of pixels	No. of floods	W^+	W^-	C	$S(c)$	C/Sc	Flood potential	AHP	AHP*C/Sc
Rainfall	32.16-68	46300	56	-0.154	0.182	-0.335	0.189	-1.772	Very Low	0.349	-0.619
	68-101	18218	18	-0.356	0.085	-0.441	0.257	-1.714	Low		-0.598
	101-147	7621	11	0.023	-0.002	0.026	0.318	0.081	Moderate		0.028
	147-209	4208	14	0.858	-0.079	0.937	0.286	3.276	High		1.143
	209-280	3068	13	1.100	-0.084	1.184	0.296	4.006	Very High		1.398
Distance from rivers	200-30845	22779	25	-0.251	0.085	-0.336	0.227	-1.481	Very Low	0.208	-0.308
	150-200	12661	7	-0.936	0.109	-1.046	0.390	-2.678	Low		-0.557
	100-150	14018			0.120	-1.025	0.367	-2.792	Moderate		-0.581
	50-100	19991	45	0.468	-0.224	0.691	0.193	3.584	High		0.745
	0-50	9966	27	0.653	-0.142	0.795	0.221	3.593	Very High		0.747
	32-68/3	7887	6	-0.617	0.050	-0.667	0.420	-1.588	Very Low		-0.203
	22-32	15127	7	-1.114	0.147	-1.261	0.390	-3.230	Low		-0.413

Slope	14-22	19116	19	-0.350	0.089	-0.439	0.252	-1.744	Moderate	0.128	-0.223
	5-14	18049	16	-0.464	0.104	-0.568	0.270	-2.102	High		-0.269
	0-5	19237	64	0.858	-0.570	1.428	0.191	7.473	Very High		0.956
Soil	Rock Outcrops/Entisols-Rock Outcrops/Inceptisols	17017	25	0.041	-0.011	0.052	0.227	0.230	Very Low	0.108	0.025
	Mollisols	28434	39	-0.028	0.015	-0.043	0.198	-0.217	Low		-0.023
	Alfisols	26154	39	0.056	-0.029	0.084	0.198	0.425	Moderate		0.046
	Inceptisols- Salt Flats	7112	8	-0.226	0.020	-0.246	0.367	-0.670	High		-0.072
	Coastal Sands- Water Body	698	1	0.016	0.000	0.016	1.005	0.016	Very High		0.002
	Areas with gypsum-lime structure	8031	5	-0.818	0.061	-0.879	0.458	-1.920	Very Low		-0.165
	Areas with conglomerate-travertine-coarse-grained texture	24560	21	-0.500	0.162	-0.663	0.242	-2.736	Low		-0.235

Geology	Areas with fine sand - mixed soils	31591	51	0.135	-0.100	0.236	0.190	1.241	Moderate	0.086	0.107
	Areas with clay soils - basalt - granite	12909	23	0.234	-0.052	0.286	0.234	1.222	High		0.105
	Areas with impermeable rock layers	2324	12	1.298	-0.084	1.381	0.306	4.511	Very High		0.388
Elevation	2843-5595	12085	8	-0.489	0.050	-0.538	0.367	-1.467	Very Low	0.059	-0.087
	2029-2843	18009	12	-0.482	0.077	-0.559	0.306	-1.830	Low		-0.108
	1244-2029	20353	16	-0.317	0.064	-0.381	0.270	-1.410	Moderate		-0.083
	488-1244	20951	31	0.316	-0.099	0.414	0.211	1.960	High		0.116
	-40-488	32398	45	0.252	-0.140	0.392	0.193	2.033	Very High		0.120
Land use	Dense forest - mountainous areas	34265	42	-0.140	0.095	-0.235	0.195	-1.203	Very Low	0.021	-0.025
	Forest lands - agriculture	10520	13	-0.132	0.019	-0.151	0.295	-0.511	Low		-0.011
	Fruit trees - agricultural lands	22141	35	0.114	-0.048	0.162	0.204	0.794	Moderate		0.017

	Herbaceous plants - groves	10564	21	0.343	-0.065	0.408	0.242	1.684	High	0.035
	Urban-coastal areas	1924	1	-0.998	0.016	-1.014	1.005	-1.009	Very High	-0.021
Flow accumulation	0-1843	77770	34	-1.171	3.515	-4.686	0.207	-22.638	Very Low	0.041	-0.928
	1843-7371	1106	27	2.851	-0.262	3.113	0.223	13.957	Low	0.572
	7371-17046	254	14	3.667	-0.130	3.797	0.293	12.961	Moderate	0.531
	17046-32249	176	15	4.104	-0.142	4.246	0.288	14.718	High	0.603
	32249-58738	110	22	4.955	-0.217	5.172	0.261	19.841	Very High	0.813

345

The risk level of each factor class was divided into five categories using Natural Breaks classification: Very Low, Low, Moderate, High, and Very High. The final susceptibility maps are shown in Fig. 3.

As indicated in Fig. 3, a large number of floods occurred near the rivers. The distribution of floods in the north of Mazandaran Basin is very dense, due to presence of plain areas and low slope in this region (Fig. 2-c, 2-g). A common feature of flood zoning maps in all three methods is the very high risk of waterways. Waterways are the main route for passing floods and are the first place of flooding risks. researches had shown that a large part of the damages in the watershed of Mazandaran province is due to the development of construction near the rivers and the lack of attention to the structures locating programs (Sadeghi-pouya et al. 2017; Rahmani et al. 2019). In all three methods, the northern areas have very high and high flood risk, which implies that these areas are very sensitive to flooding. The main difference between susceptibility map of TOPSIS-Bayesian (Fig. 3-b) with AHP-Bayesian (Fig. 3-a) and MABAC-Bayesian (Fig. 3-c) maps is in predicting the moderate level of flood risks of basin. In map (b), a large part of the basin area (39.11%) has a moderate sensitivity to flooding; While in maps (a) and (c), the areas with moderate risk is about half of the area predicted by map (b). In MABAC and TOPSIS methods, the value of each cell is calculated according to equations 12 and 16, respectively. Calculating the values of each cell will increase the accuracy in estimating flood zoning. The TOPSIS zoning map is more cohesive than the MABAC method, due to using the fuzzy method to normalize the data and reducing the difference value of cells. Therefore, a high percentage of moderate sensitivity to flooding using this method seems reasonable.

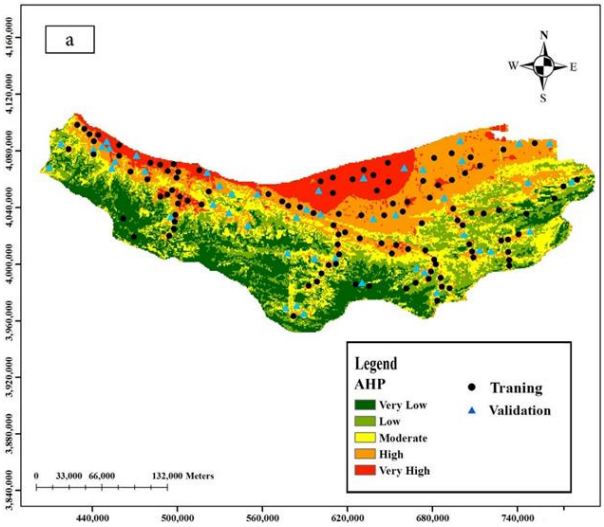

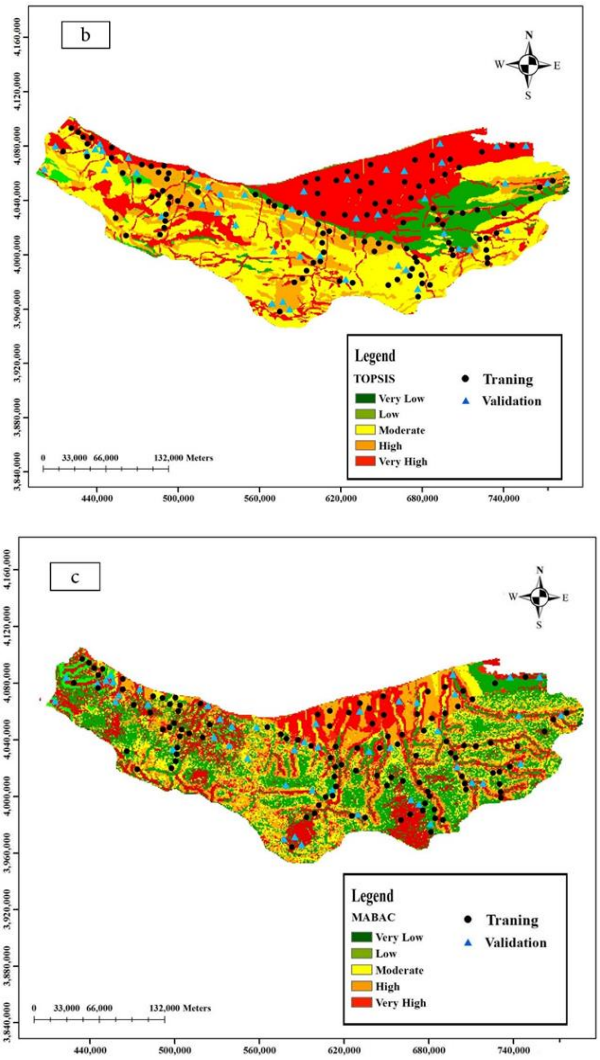

Fig. 3 Flood susceptibility maps of Mazandaran Province by combination of (a) AHP-WOE, (b) TOPSIS-AHP-WOE, and (c) MABAC-AHP-WOE

4.2. Comparison of flood susceptibility classes

According to Table 4, based on AHP-WOE method, 48.83% of the Mazandaran province was at high and very high flood risk levels. TOPSIS-WOE-AHP and MABAC-WOE-AHP methods estimated 49.34% and 41.76% of the Mazandaran province at high and very high risk levels, respectively. The MABAC-AHP-WOE method,

compared to the other two methods, has predicted the most area with low and moderate flood risk (40.39%). In general, it is concluded that this method, in comparison to the other methods, estimated the conditions of the basin in terms of the risk of future floods in a less risky situation. On the other hand, the TOPSIS-AHP-WOE, estimated a wider area of the basin (49.34%) at risk of flood damage.

Table 4 Percentage of flood risk zoning

Method	Very Low	Low	Moderate	High	Very High
AHP-WOE	20/25	9/64	21.28	29.45	19/38
TOPSIS-AHP-WOE	7/35	4/2	39.11	20/02	29/32
MABAC-AHP-WOE	36/61	3/78	17/85	23.07	18/69

Accurate verification can reassure the readers about the more accuracy of one method than the others. In the next section, the ROC method was used to validate the results.

4.3 Validation of the flood susceptibility maps

For validation of three flood susceptibility maps, the prediction rate curve was produced by 30% of the data (test data, which were not used in modeling) which contains 15 flood points. The results of the prediction rate curve are indicated in Fig. 4. The AUC value for AHP-WOE, MABAC-WOE-AHP, and TOPSIS-WOE-AHP models was 0.753 (75.3% of accuracy), 0.861 (86.1% of accuracy) and 0.916 (91.6% of accuracy), respectively. The highest degree of accuracy was for TOPSIS-WOE-AHP model due to the highest area under the curve.

It can be concluded that all the models have reasonable performance of flood prediction in the study area. Also, the TOPSIS-AHP-WOE model estimated the flood prone areas with an excellent accuracy, which indicates the high efficiency of this model.

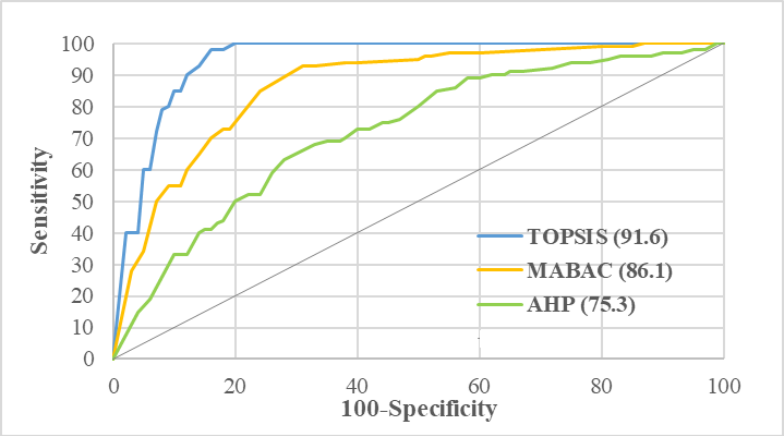

Fig. 4 The ROC curve for the flood susceptibility map of the study area using different methods

5. discussion

In Iran especially in the North, enormous floods are occurred every year. One of the most important preventive measures is preparing flood potential mapping. Thus, flood prone areas can be identified, and the proper measures can be applied to decrease flood damages. In the present study, the capability of three ensembles models based on multi criteria decision making was tested to predict the flood susceptibility in the study area.

In other studies, different kinds of multi criteria decision analysis and bivariate statics methods were applied and compare with each other. Khosravi et al. (2016) used several methods (FR, WOE, and AHP) to determine the flood susceptibility at Haraz Watershed, which located in Mazandaran Province. They indicated that all methods have a reasonable accuracy due to the high AUC value. In another study in Ethiopia, Ogato et al (2020) shows AHP method predict the flood prone areas with a high accuracy. Also, Suthirat et al. (2020) indicates that AHP-GIS flood hazard map was in good agreement with both the historical flood events and the annual maximum rainfall in Ayutthaya city in Thailand. For analyzing the flood risk in Vietnam, Luu et al. (2019) applied a TOPSIS-based method. Results revealed that the proposed model can be used for sustainable management of flood prone areas with high accuracy. Using WOE model by Rahmati et al. (2015) lead to evaluate the flood risk with reasonable result (AUC=74.74%) in Golestan Province in Iran.

Our results are in line with previous studies, which combined AHP and TOPSIS with WOE methods had high accuracy in our study area. Also, the novel proposed method (MABAC-WOE-AHP) can be useful for mapping flood potential of similar settings, due to the high performance.

Considering that a large part of the basin is in the middle to high flood hazard, Measures should be taken to manage floods. In general, the flood management cycle consists of four components: prevention, preparedness, response, and rehabilitation, and therefore, in order to apply proper management. In flood management, all aspects of the issue should be considered, from policies in development applications affecting flood intensification to coping strategies such as the construction of control structures, flood warning, evacuation, rescue, and rehabilitation measures.

6. Conclusion

One of the essential steps to reduce the harmful effects of floods is to identify flood prone areas and preparing flood susceptibility mapping. The need to have a reliable and accurate technique to determine the flood-prone areas prompted the authors to assess several methods to understand the methods' efficiency. The study focused on analyzing flooding hazards using GIS-based and the multi-criteria decision-making methods in Mazandaran Province, Iran. Therefore, combined AHP, TOPSIS, and novel MABAC methods with weight of evidence model were used. For this purpose, a flood inventory map including 160 flood locations was prepared. These locations were divided randomly into two groups of training data (112 locations) and test data (48 locations). Then, eight data layers containing rainfall, distance from rivers, slope, soil, geology, elevation, drainage density, and land use were derived from the spatial database. The results of AHP-WOE, TOPSIS-WOE-AHP, MABAC-WOE-AHP methods indicated that respectively 44.83%, 49.34%, and 41.76% of Mazandaran Province was located in high and very high risk of flooding area. Also, the MABAC-WOE-AHP method in comparison to other methods, estimated the great area (40.39%) with very low and low flood risk.

In order to validate the results of these methods, ROC curve was used for test data. The validation of the results showed that AUC value for AHP-WOE, TOPSIS-WOE-AHP, and MABAC-WOE-AHP methods was 0.753 (good accuracy), 0.916% (excellent accuracy), and 0.861% (very good accuracy), respectively. The map of this analysis was indicated the distribution of high-risk areas, which is essential for flood management strategies. Once the spatial distribution of flood hazard zoning is determined, the responsible organizations, planners, and engineers

can be more careful about preventive actions such as strengthening structures in floodplains against floods, developing flood safety guidelines, provide general education, provide flood insurance, and flood mitigation plan and implementation. For the future work, applying some machine learning models such as artificial neural network, decision trees, and support vector machine and integrated with AHP can be considered.

Conflicts of interests

The authors declare that no funding was received for conducting this study.

References

Bonham-Carter GF, Agterberg FP, Wright DF (1988) Integration of Geological Datasets for Gold Exploration in Nova Scotia. American Society for Photogrammetry and Remote Sensing. 0099-1 112.88/ 5411 – 1585$ 02.25/0

Brito M M, & Evers M (2016) Multi-criteria decision-making for flood risk management: a survey of the current state of the art. Natural Hazards and Earth System Sciences. 16(4):1019-1033

Bubeck P, Botzen W, Aerts J (2012) A review of risk perceptions and other factors that influence flood mitigation behavior. Risk Anal 32:1481–1495

Büyüközkan G, & Çifçi G (2011) A novel hybrid MCDM approach based on fuzzy DEMATEL, fuzzy ANP and fuzzy TOPSIS to evaluate green suppliers. Expert Systems with Applications. 39: 3000–3011

Choi J, Oh HJ, Lee HJ, Lee C, Lee S. 2012. Combining landslide susceptibility maps obtained from frequency ratio, logistic regression, and artificial neural network models using ASTER images and GIS. Eng Geol. 124:12–23

Costache R, Pham Q B, Sharifi E, Linh N T T, Abba, S I, Vojtek M, Vojteková J, Nhi P T T, Khoi D N (2019) Flash-Flood Susceptibility Assessment Using Multi-Criteria Decision Making and Machine Learning Supported by Remote Sensing and GIS Techniques. Remote Sensing 12, 106

Dahal RK, Hasegawa S, Nonomura A, Yamanaka M, Masuda T, Nishino K (2008) GIS-based weights-of evidence modelling of rainfall-induced landslides in small catchments for landslide susceptibility mapping. Environ Geol 54:311–324

Dalalah D, Hayajneh M, & Batieha F (2011). A fuzzy multi-criteria decision making model for supplier selection. Expert Systems with Applications. 38:8384–8391

Dang NM, Babel MS, Luong HT. 2011. Evaluation of food risk parameters in the Day River Flood Diversion Area, Red River Delta, Vietnam. Nat Hazards. 56:169–194.

Dewan A M (2013) Hazards, risk, and vulnerability. In Floods in a Megacity (pp. 35-74). Springer, Dordrecht.

Egan JP (1975) Signal detection theory and ROC analysis. Academic press

Ferna´ndez DS, Lutz MA (2010) Urban flood hazard zoning in Tucuma ´n Province, Argentina, using GIS and multicriteria decision analysis. Eng Geol 111:90–98

Gigović L, Pamučar D, Božanić D, & Ljubojević S (2017) Application of the GIS-DANP-MABAC multi-criteria model for selecting the location of wind farms: A case study of Vojvodina, Serbia. Renewable Energy. 103:501-521

Hall J, Arheimer B, Borga M, Brázdil R, Claps P, Kiss A, Llasat M C (2013) Understanding flood regime changes in Europe: a state of the art assessment. Hydrology and Earth System Sciences Discussions. 10 (12):15525-15624

Haq M, Akhtar M, Muhammad S, Paras S, Rahmatullah J (2012) Techniques of remote sensing and GIS for flood monitoring and damage assessment: a case study of Sindh province, Pakistan, Egypt. J Remote Sens Space Sci 15:135–141

Hernando D, & Romana M G (2015) Estimating the rainfall erosivity factor from monthly precipitation data in the Madrid Region (Spain). Journal of Hydrology and Hydromechanics, 63(1), 55–62

Hong H, Tsangaratos P, Ilia I, Liu J, Zhu A-X, Chen W (2018) Application of fuzzy weight of evidence and data mining techniques in construction of flood susceptibility map of Poyang County, China. Sci Total Environ 625:575–588

Hwang C L, Yoon K (1981) Methods for multiple attribute decision making. In Multiple attribute decision making (pp. 58-191). Springer, Berlin, Heidelberg

Izadikhah M, Saeidifar A, Roostaee R (2014) Extending TOPSIS in fuzzy environment by using the nearest weighted interval approximation of fuzzy numbers. Journal of Intelligent & Fuzzy Systems, 27(6): 2725-2736

Jaafari A, Najafi A, Pourghasemi HR, Rezaeian J, Sattarian A (2014) GIS-based frequency ratio and index of entropy models for landslide susceptibility assessment in the Caspian forest, northern Iran. Int J Environ Sci Te. 11(4):909–926

Jahangir M H, Reineh S M M, & Abolghasemi M (2019) Spatial predication of flood zonation mapping in Kan River Basin, Iran, using artificial neural network algorithm. Weather and Climate Extremes, 25

Jung IW, Chang H, Moradkhani H (2011) Quantifying uncertainty in urban flooding analysis considering hydro-climatic projection and urban development effects. Hydrol Earth Syst Sci 15(2):617–633

Kazakis N, Kougias I, Patsialis T (2015) Assessment of flood hazard areas at a regional scale using an index-based approach and Analytical Hierarchy Process: Application in Rhodope–Evros region, Greece. Science of the Total Environment. 538:555-563

Khosravi K, Pham B T, Chapi K, Shirzadi A, Shahabi H, Revhaug I, Bui D T (2018) A comparative assessment of decision trees algorithms for flash flood susceptibility modeling at Haraz watershed, northern Iran. Science of the Total Environment. 627:744-755

Khosravi K, Shahabi H, Pham B T, Adamowski J, Shirzadi A, Pradhan B, Hong H (2016) A comparative assessment of flood susceptibility modeling using Multi-Criteria Decision-Making Analysis and Machine Learning Methods. Journal of Hydrology. 573:311-323

Kia MB, Pirasteh S, Pradhan B, Mahmud AR, Sulaiman WNA, Moradi A (2012) An artificial neural network model for flood simulation using GIS: Johor River Basin, Malaysia. Environ Earth Sci 67:251–264

Kourgialas NN, Karatzas GP (2011) Flood management and a GIS modelling method to assess flood-hazard areas—a case study. Hydrol Sci J 56(2):212–225

Lee G, Jun K S, & Chung E S (2014) Robust spatial flood vulnerability assessment for Han River using fuzzy TOPSIS with α-cut level set. Expert Systems with Applications. 41(2):644-654

Lee MJ, Kang JE, Jeon S (2012) Application of frequency ratio model and validation for predictive flooded area susceptibility mapping using GIS. In: Geoscience and Remote Sensing Symposium (IGARSS)

Liang W, Zhao G, Wu H, & Dai B (2019) Risk assessment of rockburst via an extended MABAC method under fuzzy environment. Tunnelling and Underground Space Technology. 83: 533-544

Lin M C, Wang C C, Chen M S, Chang C A (2008) Using AHP and TOPSIS approaches in customer-driven product design process. Computers in industry. 59(1): 17-31

Lin K, Chen H, Xu C Y, Yan P, Lan T, Liu Z, & Dong C (2020). Assessment of flash flood risk based on improved analytic hierarchy process method and integrated maximum likelihood clustering algorithm. Journal of Hydrology. 584: 124696

Luu C, von Meding J, & Mojtahedi M (2019) Analyzing Vietnam's national disaster loss database for flood risk assessment using multiple linear regression-TOPSIS. International Journal of Disaster Risk Reduction. 40:101153

Malczewski J (2006) GIS-based multicriteria decision analysis: a survey of the literature. International journal of geographical information science. 20(7):703-726

Manandhar B (2010) Flood Plain Analysis and Risk Assessment of Lothar Khola, MSc Thesis, Tribhuvan University Phokara Nepal. pp. 64

Meyer V, Scheuer S, Haase D. 2009. A multicriteria approach for flood risk mapping exemplified at the Mulde river, Germany. Nat Hazards. 48:17–39.

Mohammady M, Pourghasemi HR, Pradhan B (2012) Landslide susceptibility mapping at Golestan Province, Iran: A comparison between frequency ratio, Dempster–Shafer, and weights-of-evidence models. J Asian Earth Sci. 61:221–236

Mojtahedi S M H, & Oo B L (2016) Coastal buildings and infrastructure flood risk analysis using multi-attribute decision-making. Journal of Flood Risk Management. 9(1):87-96

Morgan R P C (2005) Soil erosion and conservation (ed.). Australia: Blackwell Science Ltd.(p16)

Ogato G S, Bantider A, Abebe K, Geneletti D (2020) Geographic information system (GIS)-Based multicriteria analysis of flooding hazard and risk in Ambo Town and its watershed, West shoa zone, oromia regional State, Ethiopia. Journal of Hydrology: Regional Studies. 27:100659

Ohlmacher GC, Davis JC (2003) Using multiple logistic regression and GIS technology to predict landslide hazard in northeast Kansas, USA. Eng Geol 69:331–343

Ouma YO, Tateishi R (2014) Urban flood vulnerability and risk mapping using integrated multi-parametric AHP and GIS: methodological overview and case study assessment. Water 6(6):1515–1545

Pamučar D, & Ćirović G (2015) The selection of transport and handling resources in logistics centers using Multi-Attributive Border Approximation area Comparison (MABAC). Expert systems with applications. 42(6): 3016-3028

Pourghasemi HR, Pradhan B, Gokceoglu C (2012) Application of fuzzy logic and analytical hierarchy process (AHP) to landslide susceptibility mapping at Haraz watershed, Iran. Nat Hazards 63(2):965–996

Pourghasemi HR, Pradhan B, Gokceoglu C, Deylami Moezzi K (2013) A comparative assessment of prediction capabilities of Dempster-Shafer and Weights-of-evidence models in landslide susceptibility mapping using GIS. Geomat Nat Hazards Risk. 4(2):93–118

Pourghasemi HR, Moradi HR, Aghda SMF, Gokceoglu C, Pradhan B. (2014) GIS-based landslide susceptibility mapping with probabilistic likelihood ratio and spatial multi-criteria evaluation models. Arab J Geosci. 7(5):1857-1878

Pourtaghi ZS, Pourghasemi HR. (2014) GIS-based groundwater spring potential assessment and mapping in the Birjand Township, southern Khorasan Province, Iran. Hydrogeol J. doi: 10.1007/s10040-013-1089-6

Pradhan B, Lee S, Mansor S, Buchroithner MF, Jallaluddin N, Khujaimah Z (2008) Utilization of optical remote sensing data and geographic information system tools for regional landslide hazard analysis by using binomial logistic regression model. J Appl Remote Sens. 2:1–11

Pradhan B, Mansor S, Pirasteh S, Buchroithner M (2011) Landslide hazard and risk analyses at a landslide prone catchment area using statistical based geospatial model. Int J Remote Sens 32(14):4075–4087

Radmehr A, & Araghinejad S (2014) Developing strategies for urban flood management of Tehran city using SMCDM and ANN. Journal of Computing in Civil Engineering. 28(6):05014006

Rahman, M., Ningsheng, C., Islam, M. M., Dewan, A., Iqbal, J., Washakh, R. M. A., & Shufeng, T. (2019). *Flood Susceptibility Assessment in Bangladesh Using Machine Learning and Multi-criteria Decision Analysis.* Earth Systems and Environment

Rahmani sh, Azizian A, Samadi A (2019) New Method for Flood Hazard Mapping in GIS (Case Study: Mazandaran Province Sub-Basins). Iran-Water Resources Research. 15(3):339-343

Rahmati O, Nazari Samani A, Mahdavi M, Pourghasemi HR, Zeinivand H (2014) Groundwater potential mapping at Kurdistan region of Iran using analytic hierarchy process and GIS. Arab J Geosci. doi: 10.1007/s12517-014-1668-4

Rahmati O, Pourghasemi HR, Zeinivand H (2015) Flood susceptibility mapping using frequency ratio and weights-of-evidence models in the Golastan Province, Iran. Geocarto Int.

Rimba AB, Setiawati MD, Sambah AB Miura F (2017) Physical Flood Vulnerability Mapping Applying Geospatial Techniques inOkazaki City,AichiPrefecture, Japan. Urban Sci1(7):1–22

Saaty T L (1977) A scaling method for priorities in hierarchical structures. Journal of mathematical psychology. 15(3):234-281

Sadeghi-Pouya A, Nouri J, Mansouri N, & Kia-Lashaki A (2017) An indexing approach to assess flood vulnerability in the western coastal cities of Mazandaran, Iran. International journal of disaster risk reduction. 22:304-316

Shafapour Tehrany M, Shabani F, Neamah Jebur M, Hong H, Chen W, Xie X (2017) GIS-based spatial prediction of flood prone areas using standalone frequency ratio, logistic regression, weight of evidence and their ensemble techniques. Geomat Nat Hazards Risk 8:1538–1561

Subramanian N, & Ramanathan R (2012) A review of applications of Analytic Hierarchy Process in operations management. International Journal of Production Economics. 138(2):215-241

Suthirat K, Athit P, Patchapun R, Brundiers K, Buizer J L, & Melnick R (2020). AHP-GIS analysis for flood hazard assessment of the communities nearby the world heritage site on Ayutthaya Island, Thailand. International Journal of Disaster Risk Reduction. 101612

Tehrany M S, Pradhan B, Jebur M N (2015) Flood susceptibility analysis and its verification using a novel ensemble support vector machine and frequency ratio method. Stochastic Environmental Research and Risk Assessment, 29(4):1149-1165

Xu C, Xu X, Dai F, Xiao J, Tan X, Yuan R (2012) Landslide hazard mapping using GIS and weight of evidence model in Qingshui river watershed of 2008 Wenchuan earthquake struck region. J Earth Sci 23:97–120

Yeon YK, Han JG, Ryu KH. 2010. Landslide susceptibility mapping in Injae, Korea, using a decision tree. Eng Geol. 116:274–283

Yesilnacar EK. (2005) The application of computational intelligence to landslide susceptibility mapping in Turkey. Ph.D Thesis Department of Geomatics the University of Melbourne 423 pp

Youssef AM, Pradhan B, Pourghasemi HR, Abdullahi S (2015) Landslide susceptibility assessment at Wadi Jawrah Basin, Jizan region, Saudi Arabia using two bivariate models in GIS. Geosci J. doi:10.1007/ s12303-014-0065-z

Zhu F, Zhong P A, & Sun Y (2018) Multi-criteria group decision making under uncertainty: Application in reservoir flood control operation. Environmental modelling & software. 100:236-251

Zou Q, Zhou J, Zhou C, Song L, Guo J (2013) Comprehensive flood risk assessment based on set pair analysis-variable fuzzy sets model and fuzzy AHP. Stoch Environ Res Risk Assess 27(2):525–546

606

607

Figures

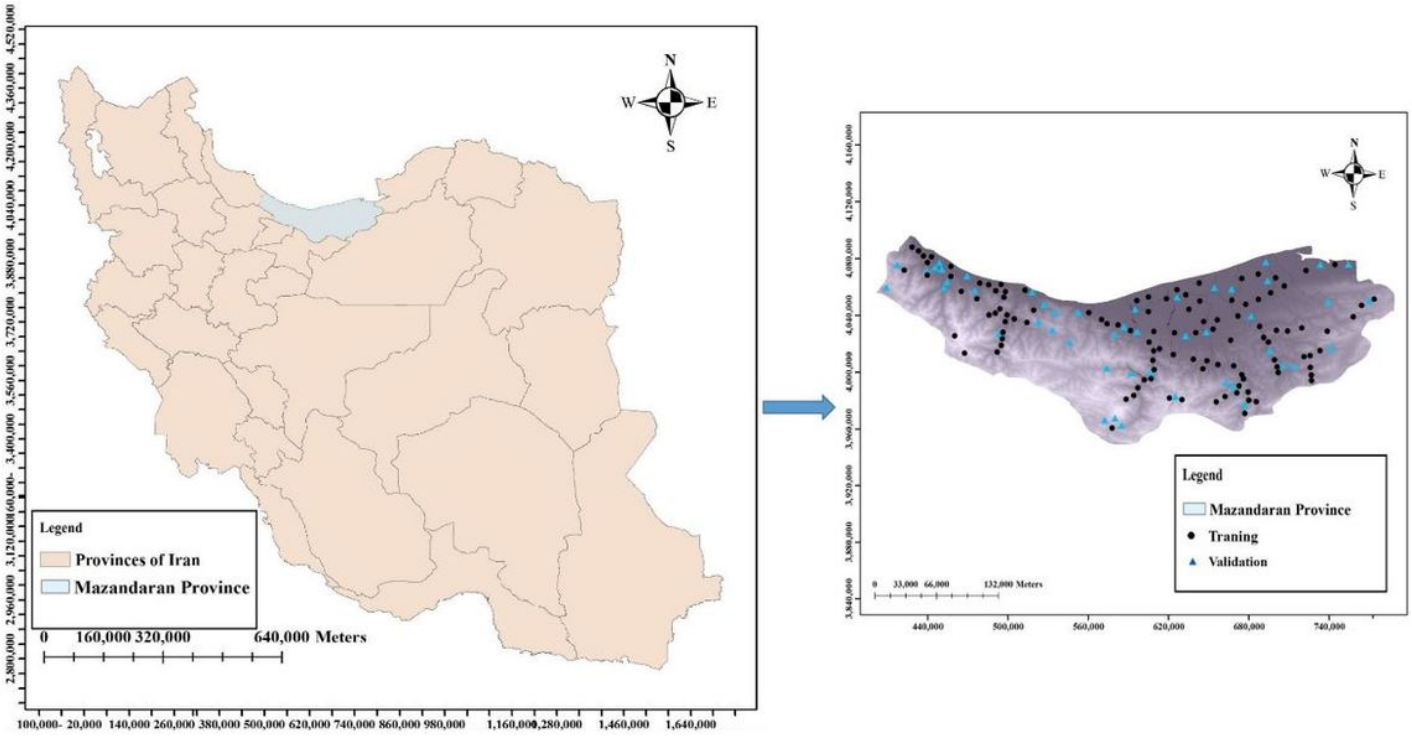

Figure 1

Flood location map of Mazandaran Province, Iran Note: The designations employed and the presentation of the material on this map do not imply the expression of any opinion whatsoever on the part of Research Square concerning the legal status of any country, territory, city or area or of its authorities, or concerning the delimitation of its frontiers or boundaries. This map has been provided by the authors.

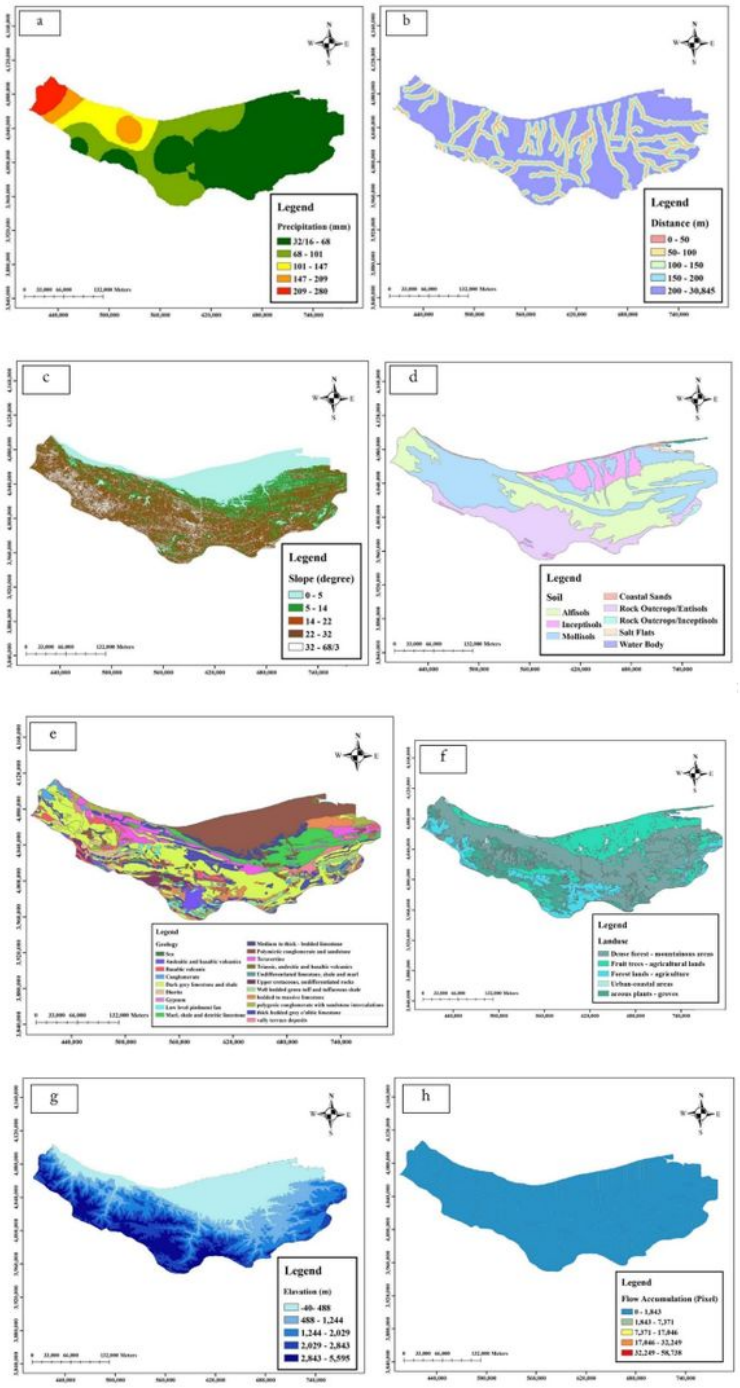

Figure 2

Flood conditioning factors in the study area: (a) rainfall (b) distance from rivers (c) slope (d) soil type (e) geology (f) land use (g) elevation (h) flow accumulation Note: The designations employed and the presentation of the material on this map do not imply the expression of any opinion whatsoever on the part of Research Square concerning the legal status of any country, territory, city or area or of its

authorities, or concerning the delimitation of its frontiers or boundaries. This map has been provided by the authors.

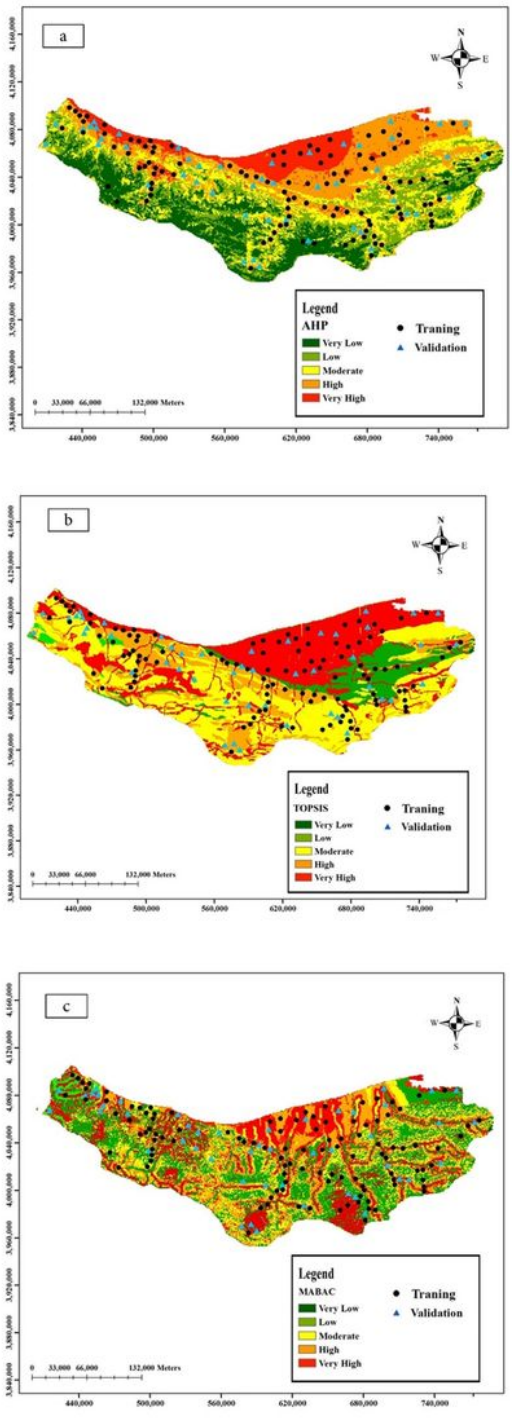

Figure 3

Flood susceptibility maps of Mazandaran Province by combination of (a) AHP-WOE, (b) TOPSIS-AHP-WOE, and (c) MABAC-AHP-WOE Note: The designations employed and the presentation of the material on this map do not imply the expression of any opinion whatsoever on the part of Research Square

concerning the legal status of any country, territory, city or area or of its authorities, or concerning the delimitation of its frontiers or boundaries. This map has been provided by the authors.

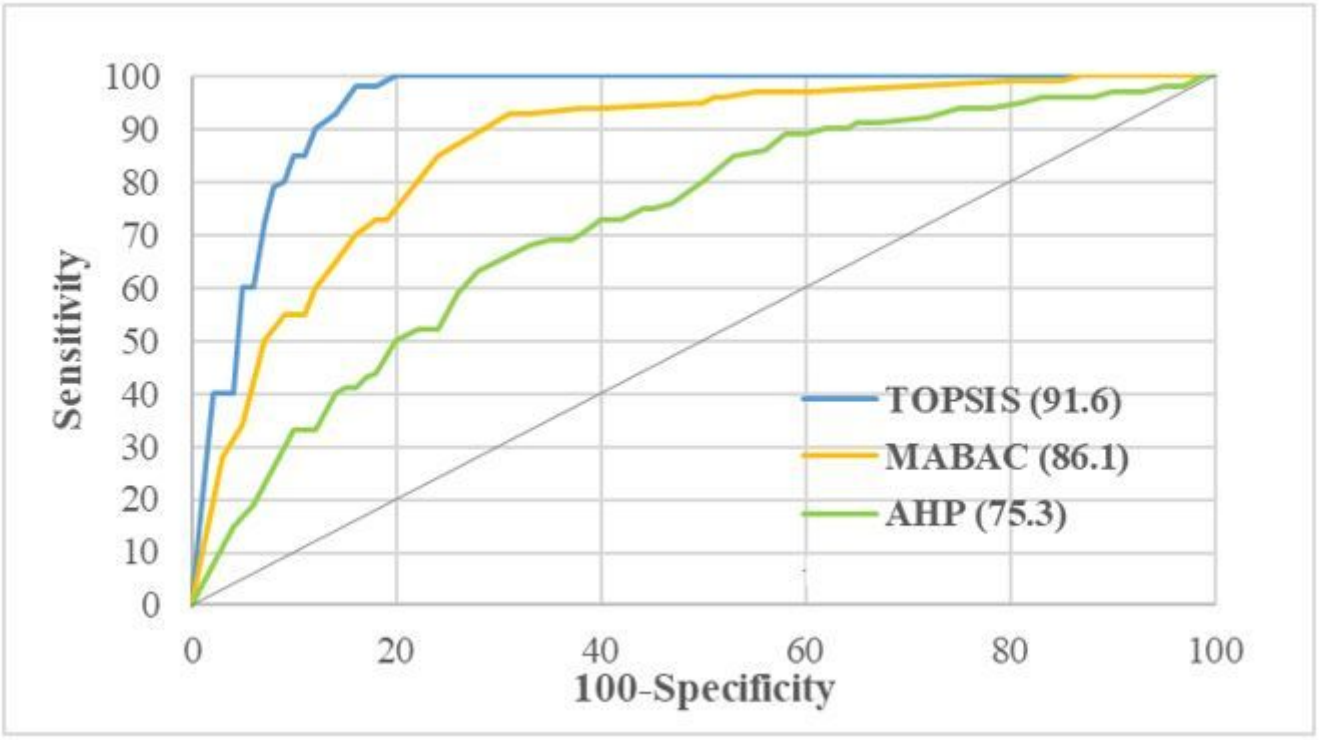

Figure 4

The ROC curve for the flood susceptibility map of the study area using different methods